

# **Focused laser beams and liquid crystals: fast three-dimensional imaging of structures and topological defects**



## 2. EXPERIMENTAL TECHNIQUES

### 2.1. Experimental set up of the Fast FCPM

The recent development in the field of fast-scanning microscopy allows one to increase the rate of confocal imaging by three-to-four orders of magnitude, i.e., up to about 1000 frames per second<sup>5</sup>. This fast confocal imaging system is based on the principle of the rotating Nipkow disk with thousands of pinholes, a very old (1884) invention, used in early-stages television. The modern addition<sup>5</sup> is that the Nipkow disk with pinholes is supplemented by a coaxial disk with micro-lenses. The two discs are mechanically connected and are rotated together by an electrical motor. The micro-lenses focus light onto the pinholes, so that the sample is scanned by thousands of beams at once allowing to increase the speed of imaging by orders of magnitude. The Fast FCPM set up, Fig.1b, is based on the scanning system with a spinning dual Nipkow disk with 20,000 of pinholes and micro-lenses integrated with a Nikon microscope Eclipse E-600 POL base. The microscope is equipped with an accurate (50 nm in setting the vertical position of the focused beam) focus drive. The excitation can be performed in the spectral range between 300 and 900 nm (mercury lamp). The vertical refocusing is performed by a fast piezo z-stepper (PI Piezo) capable of scanning a 10 micron-thick sample by producing 10 frames in less than 5 ms. For repetitive processes, one can use only xy-scanning, refocusing it at different depth step-by step. The speed of imaging depends on many additional factors, such as needed contrast (integration time), size of the scanned area, camera and software, but in majority of situations it can reach 1000 frames per second.

## **2.2. Basic principles of FCPM imaging**



samples was within the range 70-80% by weight. The lyotropic lamellar LC was studied in rectangular glass capillaries. The untreated glass of the capillaries sets boundary conditions at the liquid crystal-glass interface for the lamellae of the ternary system to orient parallel to the interface. In most parts of the sample the lamellae are parallel to the confining substrates. The observed deformations in the layers structure are in the form of the so-called focal conic domains (FCDs). The 3D configuration of the director  $\hat{n}$  inside the domain is rather complex; the important feature of this structure is that any line that connects a point on the ellipse to a point on the hyperbola, is the local optic axis. FCPM allows one to clearly reconstruct the basic features of this pattern. Figure 4 shows both “horizontal” (parallel to the ellipse, Fig.4a,b) and “vertical” (parallel to the hyperbola, Fig.4d,e) cross-sections of the domains. The FCPM in-plane cross-sections are co-localized with a polarizing microscopy image of the same part of the sample, Fig.4c.

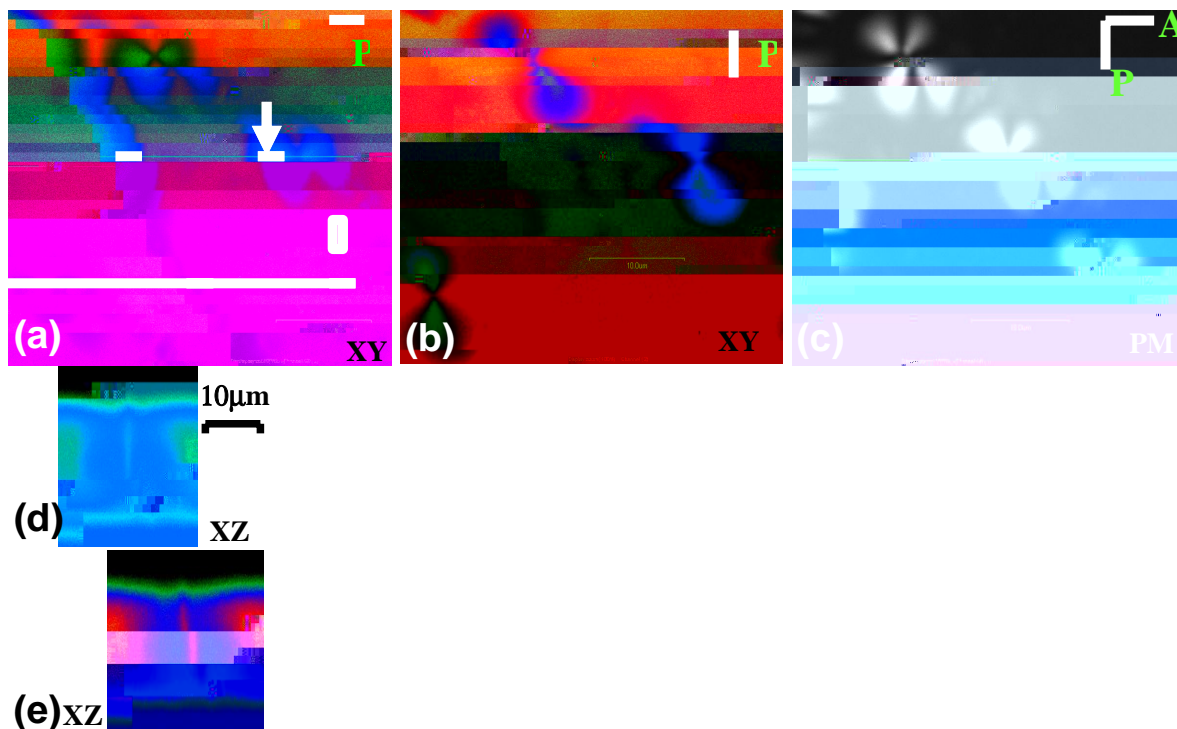


Fig. 4. Focal Conic Domains in the lyotropic  $L_\alpha$ -phase of the ternary system cetylpyridinium chloride-hexanol-brine: (a,b) in-plane FCPM cross-sections for different orientations of polarizer P; (c) PM texture of the same part of the LC cell; (d,e) FCPM vertical cross-sections of the focal conic domains marked by “d” and “e” in (a), respectively; (f) schematic illustration of the alignment of the transition dipoles of the DiOC<sub>18</sub>(3) dye molecules parallel to the lamellae in the lyotropic  $L_\alpha$ -phase; (g) layered structure of a focal conic domain different cross-sections of which are visualized by the FCPM in parts (a,b,d,e). The color-coded intensity scale of the fluorescence signal in FCPM is the same as in Fig.3.

We used dye DiOC<sub>18</sub>(3) in which the transition dipole aligns parallel to the lamellae in the lamellar  $L_\alpha$  phase of lyotropic ternary system cetylpyridinium chloride (CPCL), hexanol and brine (water +1% NaCl). The observation that the molecules of DiOC<sub>18</sub>(3) align with their transition dipoles parallel to lamellae is similar to the prior study for the case of other lyotropic lamellar systems<sup>20</sup>. As expected for such dye alignment, the fluorescence signal from the parts of cell in which the lamellae are parallel to substrates is much stronger than from the parts of cell in which layers are nearly perpendicular to the cell substrates, Fig.4. In the parts of cell with chains of focal conic domains the fluorescence signal is lower as compared to the homeotropic parts of cell. The appearance of the FCDs changes with rotation of the polarizer (compare parts (a) and (b) in Fig.4) similarly to the case of FCDs in thermotropic smectics,<sup>6, 8</sup> but now the stronger fluorescence intensity corresponds to unperturbed homeotropic part of the cell rather than to the regions with FCDs. We stress again that this is due to the fact that the DiOC<sub>18</sub>(3) dye molecules orient parallel to the planes of the

lamellae, Fig.4f, not along the layer normal, director  $\hat{n}$ , as in the case of thermotropic smectic<sup>6</sup>. Figure 4g shows a typical layered structure of the focal conic domain that can be reconstructed from the FCPM images, Fig.4a,b,d,e. Note that in Fig.4, the base of FCD is located in the bulk of the lamellar sample; in thermotropic smectic A samples, surface anchoring might cause the bases of FCDs to be located at the boundary<sup>8</sup>.

### **3.2. Dynamics of defects and director structures.**

The examples of the 3D imaging provided above correspond to the static director structures in which the director field is spatially complex but does not change with time, at least on the time scale of hours which is much larger than the time needed to acquire the FCPM images by both types of confocal microscopes shown in Fig.1. The vertical

isotropic phase above  $\sim 35^{\circ}\text{C}$ . When the sample is cooled down, solubility of glycerol in 5CB decreases and one observes appearance and growth of glycerol droplets. The technique produces droplets of a practically constant radius in the films of controlled thickness which is in the range  $h=(1-100)$  microns. The size of droplets is controlled by the cooling rate and thermal cycling. The 5CB film is in the so-called hybrid aligned state, as the director  $\hat{n}$  is parallel to the LC-glycerol interface at the bottom and perpendicular to the air-LC interface at the top.

Fig.6. FCPM vertical cross-section of a glycerol droplet at the liquid crystal-air interface: (a) fluorescence from glycerol doped with fluorescein; (b) polarized fluorescence signal from the liquid crystal doped with the Nile Red dye.

Two different dyes with well separated absorption and fluorescence bands, fluorescein and Nile red (both purchased from Aldrich), were added in small quantities (0.01 wt %) to tag glycerol and LC, respectively. The molecules of fluorescein are relatively polar and their solubility in glycerol is much better than in LC. Therefore, after the phase separation of glycerol and LC, the Fluorescein molecules stay in glycerol, which are also polar and contain similar hydroxyl groups as the dye molecules. The molecules of Nile Red have hydrophobic tails and anisometric shape,



7b shows spatial displacements from their original positions (taken to be at the origin of the coordinate system) of the bead during constant periods of time (15miliseconds); the corresponding histograms for each coordinate are shown in Fig.7c,d. As the particle undergoes Brownian motion, the director distortions around it on average retain quadrupolar symmetry, Fig.7a.

Fig.7. (a) In-plane FCPM texture of director distortions around a spherical particle of  $3\mu\text{m}$  diameter with tangential anchoring; (b) the displacement of the particles undergoing Brownian motion in the plane of the cell, (c,d) the corresponding histograms for each coordinate. The far- friihen (m pak12(esed3( fob12(esy)i)-10(ons) d the u12(esb)( )14(In-pe10(ons)-13( )14(B)the w3( fo)-15(l)d3( fo“[(acjET1Q BT/)]TJ0.0

the inter-particle-separation is larger than 3-4 particle diameters, but the anisotropic colloidal interactions become noticeable at smaller separations. The attracting particles eventually touch at about 30 degrees with respect to the far-field uniform director  $\hat{a}$ . Figure 8c illustrates the trajectories of particle motion in the liquid crystal matrix as they attract each other. For the detailed study of colloidal interactions and aggregation of particles with tangential anchoring we refer the reader to Ref. <sup>22</sup>

#### 4. CONCLUSION

The examples above illustrate that the Fluorescence Confocal Polarizing Microscopy can be successfully used for many problems in different soft matter systems, whenever one is interested in orientational features of molecular organization. Using special dyes and polarized light, one can get an access not only to the spatial positional 3D pattern, but also to the 3D pattern of molecular orientation. We showed that FCPM can be used not only in the studies of relatively simple and spatially homogeneous samples (in terms of composition), but also in the studies of heterogeneous systems, such as nematic emulsions and colloidal suspensions. We also demonstrated that FCPM is capable of hetero-

9. I. I. Smalyukh and O. D. Lavrentovich, "Three-dimensional director structures of defects in Grandjean-Cano wedges of Cholesteric liquid crystals studied by fluorescence confocal polarizing microscopy," *Phys. Rev. E* **66**, 051703/1-16 (2002).
10. I. I. Smalyukh and O. D. Lavrentovich, "Anchoring-mediated interaction of edge dislocations with bounding surfaces in confined cholesteric liquid crystals," *Phys. Rev. Lett.* **90**, 085503/1-4 (2003).
11. B. I. Senyuk, I. I. Smalyukh, O. D. Lavrentovich, "Switchable two-dimensional gratings based on field-induced